BRIEF REPORT

Resolving Complex Structural Variants in Undiagnosed Rare Movement Disorders via Multimodal Genomics and Multi-omics

Ugo Sorrentino, MD,[1,2*] Melanie Brugger, MD,[1] Alice Saparov, MSc,[1,2] Ivana Dzinovic, PhD,[1,2] Philip Harrer, MD, PhD,[1,2] Sandy Lösecke,[1] Kevork Derderian, MSc,[1] Martin Pavlov, MSc,[1,2] Robert Kopajtich, MSc,[1,2] Holger Prokisch, PhD,[1,2,3] Arcangela Iuso, PhD,[1,2] Maria Mazurkiewicz-Bełdzińska, MD,[4] Deike Weiss, MD,[5] Christina Ludwig, PhD,[6] Miriam Abele, PhD,[6] Julia Mergner, PhD,[7] Juliane Winkelmann, MD,[1,2,8,9] Theresa Brunet, MD,[1] Michał Schinwelski, MD,[10,11] Elisabeth Graf, PhD,[1] Katja Kloth-Stachnau, MD,[12] Theresia Herget, MD,[13] Magdalena Krygier, MD, PhD,[4] and Michael Zech, MD[1,2,14]

ABSTRACT: Background: Long-read sequencing and multi-omic analytical frameworks are increasingly being adopted in rare disease diagnostics. However, clinical workflows comprehensively integrating these methodologies remain uncommon.

Objective: This study aimed to assess the potential and limitations of integrating long-read genomic, transcriptomic, and proteomic analyses to characterize complex structural variants.

Methods: Two unrelated patients presenting with dystonia and comorbid neurological features underwent nanopore-based long-read DNA sequencing. In patient 1, complementary transcriptomic and proteomic analyses were performed.

Results: The workflow enabled the identification and characterization of two pathogenic complex structural variants: a homozygous AluY-mediated inversion disrupting *PANK2*, underlying neurodegeneration with brain iron accumulation (patient 1), and a heterozygous de novo 16p13.3 duplication-triplication event associated with an atypical dystonia-parkinsonism phenotype (patient 2).

Conclusions: Our findings underscore the diagnostic potential of integrated long-read and multi-omic approaches for complex structural variant characterization, while illustrating persistent limitations of automated pipelines and highlighting unpredictable relationships between genomic, transcriptomic, and proteomic findings. © 2026 The Author(s). *Movement Disorders* published by Wiley Periodicals LLC on behalf of International Parkinson and Movement Disorder Society.

Key Words: complex structural variants; dystonia; long-read sequencing; multi-omics; nanopore technology

[1]Institute of Human Genetics, School of Medicine and Health, Technical University of Munich, Munich, Germany; [2]Institute of Neurogenomics, Helmholtz Zentrum München, Munich, Germany; [3]Deutsches Zentrum für Kinder- und Jugendgesundheit, Munich, Germany; [4]Department of Developmental Neurology, Medical University of Gdansk, Gdansk, Poland; [5]Department of Pediatrics, University Medical Center Hamburg-Eppendorf, Hamburg, Germany; [6]Bavarian Center for Biomolecular Mass Spectrometry (BayBioMS), Technical University of Munich, Freising, Germany; [7]Bavarian Center for Biomolecular Mass Spectrometry at the University hospital rechts der Isar, Technical University of Munich, Munich, Germany; [8]DZPG, Deutsche Zentrum für Psychische Gesundheit, Munich, Germany; [9]Munich Cluster for Systems Neurology, Munich, Germany; [10]Division of Neurological and Psychiatric Nursing, Faculty of Health Sciences, Medical University of Gdańsk, Gdansk, Poland; [11]Neurocentrum-Miwomed Sp. z o.o, Gdańsk, Poland; [12]Amedes MVZ für Humangenetik Hamburg GmbH, Hamburg, Germany; [13]Institute of Human Genetics, University Medical Center Hamburg-Eppendorf, Hamburg, Germany; [14]Institute for Advanced Study, Technical University of Munich, Garching, Germany

*__Correspondence to:__ Dr. Ugo Sorrentino, Institute of Human Genetics at the Klinikum Rechts of Isar, Trogerstraße 32, 81675 Munich, Germany; E-mail: ugo.sorrentino@mri.tum.de

Relevant conflicts of interest/financial disclosures: Author disclosures are available in the Supporting Information.

Funding agencies: This work was supported by a "*Schlüsselprojekt*" grant from the Else Kröner-Fresenius-Stiftung (2022_EKSE.185). This research was also supported by funding from EJP RD (EJP RD Joint Transnational Call 2022) and the German Federal Ministry of Education and Research (BMBF, Bonn, Germany), awarded to the project PreDYT (PREdictive biomarkers in DYsTonia, 01GM2302). In addition, this study (M.Z.) has received funding from the BMBF and the Free State of Bavaria under the Excellence Strategy of the Federal Government and the Länder, as well as by the Technical University of Munich – Institute for Advanced Study. H.P. acknowledges grant support from the BMBF, awarded to the German Network for Mitochondrial Disorders (mitoNET, 01GM1906A), and also received grant support from the EJP RD and the BMBF, awarded to the GENOMIT project (01GM2301 and 01GM2404A). The Orbitrap Fusion Lumos mass spectrometer was supported by the German Research Foundation (INST 95/1436-1 FUGG).

Received: 28 April 2026; **Revised:** 19 June 2026; **Accepted:** 24 June 2026

Published online in Wiley Online Library (wileyonlinelibrary.com). DOI: 10.1002/mds.70427

A considerable proportion of movement disorders has been attributed to highly heterogeneous monogenic etiologies, both in pediatric and adult patient populations.[1-3] Since their introduction into clinical practice, high-throughput short-read sequencing technologies have been regarded as the gold standard approach for the molecular diagnosis of such conditions.[4-6] Nevertheless, the diagnostic yield of genetically heterogeneous movement disorder syndromes remains comparatively modest relative to the number of cases in which a single-gene etiology would be clinically anticipated.[7] In addition to an incomplete understanding of causally associated genes and their underlying pathogenic mechanisms, well-established factors also contribute to diagnostic gaps: (1) the intrinsic limitations of short-read sequencing in detecting certain categories of genomic alterations,[8,9] and (2) the often insufficient predictive and classificatory power of genomic sequence data alone in establishing pathogenicity.[10-12] In this context, long-read genome sequencing (lrGS)and multiomic approaches are expected to improve the diagnosis of monogenic disorders by better characterizing genomic variants and their downstream molecular consequences.[9,13-18] However, successful and reproducible clinical applications combining long-read genomics, short- and long-read transcriptomics (short-read [srRNAseq] and long-read RNA sequencing [lrRNAseq]), and proteomics remain seldomly described in the published literature.[19-21]

In this study, we report the diagnostic workup of two unrelated patients presenting with complex forms of dystonia, in whom standard short-read sequencing had failed to yield a definitive molecular diagnosis. Through long-read DNA sequencing, complemented by transcriptomic and proteomic analyses in the first patient, we identified and characterized two pathogenic complex structural variants (cxSVs): a *PANK2*-disrupting homozygous inversion underlying neurodegeneration with brain iron accumulation (NBIA; Online Mendelian Inheritance in Man [OMIM] 234200), and a heterozygous de novo 16p13.3 duplication-triplication event associated with an atypical dystonia-parkinsonism phenotype.[22]

Subjects and Methods

See Supporting Information Methods for details.

Results

Patient 1: *PANK2*-Related NBIA

The first patient, a 19-year-old woman, showed a complex phenotype characterized by psychomotor delay, absent language, dystonia, and brain imaging compatible with *PANK2*-related NBIA. Further details are reported in the Supporting Information Results.

Trio exome sequencing (ES), including detailed evaluation and reevaluation of the *PANK2* locus, failed to identify any pathogenic or likely pathogenic variant (Fig. S1A). Parallel srRNAseq and trio short-read whole genome sequencing (srWGS) were initiated to further investigate the *PANK2* locus. srRNAseq demonstrated a significant splicing outlier (adjusted $P = 0.026804$; delta psi: -0.32), while expression outlier analysis did not reach statistical significance; sample-level ranking nonetheless indicated reduced *PANK2* expression, approximately consistent with monoallelic levels (Fig. S2A,B). Read-alignment and Sashimi-plot inspection of srRNAseq data identified a marked reduction in read coverage at the exon 4–5 junction (Fig. S2C,D), and closer examination showed that the residual reads mapping to this junction were, in fact, misaligned, originating from a distinct locus on chromosome 20 (Fig. S2E). Concordantly, srWGS showed a homozygous 9.65-Mb stretch on chromosome 20p13 (Fig. S3). Within this region, a subset of implemented structural variant (SV) callers indicated the presence of an inversion of approximately 1.265 Mb, providing a potential genomic correlate for the transcriptomic findings. However, breakpoint resolution and unambiguous variant identity could not be established from short-read data. The putative breakpoints were localized to two highly homologous short interspersed nuclear elements of the AluY subfamily: one residing within *PANK2* intron 4 and the other in the intergenic region between *TMC2* and *NOP56* (Fig. S1B). The rearrangement was predicted to divide the *PANK2* gene into two discrete segments: one comprising exon 1 through a portion of intron 4 (containing exons 1–4 of the canonical transcript NM_001386393.1), and the other encompassing the remainder of intron 4 through exon 7 (containing exons 5–7). In both parents, the srWGS result was consistent with a heterozygous carrier state.

Given the complexity of the variant, ONT-based lrGS was performed to refine breakpoint resolution, confirm the inversion architecture, and verify zygosity. Interestingly, the automated SV calling algorithms integrated into the Oxford Nanopore Technologies (ONT) pipeline (Spectre and Sniffles2, with the later addition of the alternative tool CuteSV for validation) failed to detect the inversion. Conversely, manual inspection of the lrGS data enabled a more accurate delineation of the breakpoints of the homozygous inversion and provided a clearer visual representation of the involvement of the two AluY elements (Fig. 1A). The spatial configuration of the two AluY elements, located at (GRCh38/hg38) chr20:2648550–2648648 and chr20:3913791–3914088, was consistent with nonallelic homologous recombination as the underlying mutational mechanism, with these

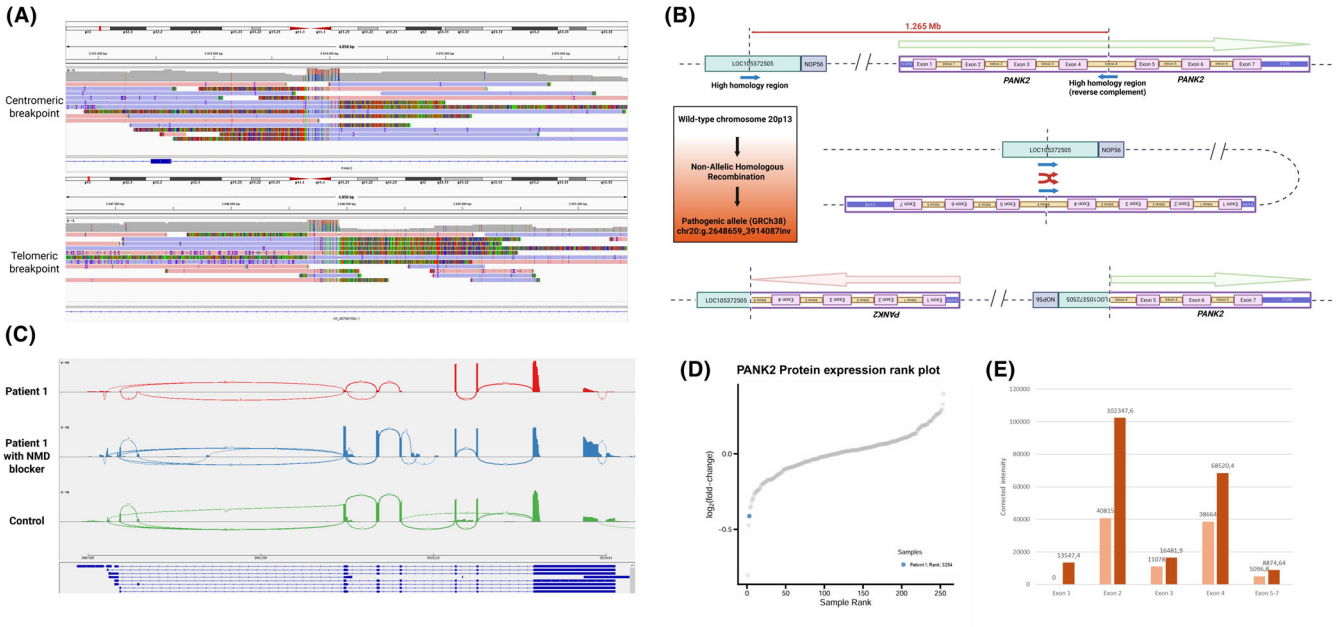

FIG. 1. Multi-omic characterization of the homozygous *PANK2*-disrupting inversion at chromosome 20p13. (**A**) Integrative Genomics Viewer (IGV)[23] visualization of ONT long-read genome sequencing (lrGS) data from patient 1 at the centromeric (top) and telomeric (bottom) inversion breakpoints. Soft-clipped reads were concentrated around two highly homologous AluY sequences, enabling manual delineation of the breakpoints. Detailed annotation and interpretation of the read alignments are provided in Supporting Information Figure S4. (**B**) Schematic representation of the structural rearrangement at the *PANK2* locus. The wild-type chromosome 20p13 configuration (top) harbored two highly homologous AluY elements in reverse complement orientation, with the centromeric element located within the *PANK2* locus. Nonallelic homologous recombination (NAHR) between these elements was proposed as the mechanism underlying the ~1.265-Mb inversion (pathogenic allele, GRCh38: chr20:g.2648659_3914087inv), which divided *PANK2* into two discrete, noncontiguous segments on the rearranged chromosome (bottom). (**C**) Sashimi plot of the lrRNAseq data from the same three samples, illustrating the exon connectivity patterns of the detected transcript isoforms. The complete absence of reads spanning the exon 4–5 junction confirmed the lack of full-length *PANK2* transcripts in patient 1. Residual isoforms encompassing exclusively exons 5, 6, and 7 were detectable in the nonsense-mediated decay (NMD)-uninhibited condition and appeared overrepresented relative to the NMD-inhibited condition, suggesting active transcriptional production rather than passive NMD escape. (**D**) PROTRIDER rank plot of PANK2 protein abundance across 254 internal proteomics samples from subjects with rare diseases. Patient 1 ranked among the lowest-expressing samples (rank 3/254), indicating reduced overall PANK2 protein abundance, although not reaching statistical significance as a formal expression outlier. The sample with the lowest PANK2 expression had a confirmed diagnosis of *PANK2*-related neurodegeneration with brain iron accumulation (NBIA; biallelic pathogenic variants), while the individual ranked second to lowest carried a single heterozygous pathogenic *PANK2* variant, providing further contextual support for the clinical relevance of the observed expression reduction in patient 1. (**E**) Bar plot of peptide signal intensities corresponding to individual *PANK2* exons in patient 1 fibroblasts (light bars) compared with the aggregated mean of 10 control samples from the same batch (dark bars). Peptides encoded by exon 1 were undetectable in patient 1. Peptide intensities corresponding to exons 2 to 4 were markedly reduced relative to controls, while those corresponding to exons 5 to 7 showed a comparatively lesser reduction, consistent with the residual exon 5 to 7 transcriptional activity detected by lrRNAseq. No peptide signals corresponding to an exon 5– to exon 7–specific isoform was identified above background levels. UTR, untranslated region. [Color figure can be viewed at wileyonlinelibrary.com]

sites representing the most probable recombination substrates driving the rearrangement (Figs. 1B and S4).

To further resolve the apparent discrepancy between a homozygous frame-disrupting inversion and the absence of a significant reduction in overall *PANK2* mRNA expression (approximately 78% of the control mean; $\log_2$ fold-change: −0.3479758), we performed lrRNAseq and proteomic analysis to characterize the residual transcriptomic and translational output at the *PANK2* locus. lrRNAseq confirmed the complete absence of full-length *PANK2* transcripts. Residual transcriptional activity was nonetheless detected under both nonsense-mediated decay (NMD)-inhibited and uninhibited conditions, comprising at least three truncated isoforms derived from the 5′ segment and, unexpectedly, one isoform encompassing exclusively exons 5, 6, and 7 (Figs. 1C and S5). The exons 5 to 7 isoform was notably overrepresented in the NMD-uninhibited relative to the NMD-inhibited condition, suggesting active transcriptional production rather than passive NMD escape; alternatively, stress responses induced by cycloheximide treatment may have comparatively reduced the production of this isoform.

The detection of still preserved, although truncated, isoforms provided an explanation to the nonsignificant expression outlier readout by OUTRIDER, which aggregates reads across all annotated exons of a gene but is not able to discriminate between truncated nonfunctional transcripts and full-length productive ones. Proteomic analysis corroborated the transcriptomic findings, demonstrating reduced overall PANK2 protein abundance in the patient sample at a magnitude broadly comparable with that observed at the transcript level, although not reaching statistical significance as a formal expression outlier (Fig. 1D,E). However, the relative overabundance of the exons 5 to 7 isoform

detected by lrRNAseq was not reflected by a corresponding increase at the peptide level (Table S1). One possible explanation could be linked to the presence, in the truncated transcript, of a short sequence derived from the inverted segment, which corresponds to the first exon of an uncharacterized noncoding RNA (LOC105372505): the inclusion into the transcript of a sequence not meant to be translated could affect the stability of the 5′ end of the fusion isoform, possibly leading to inefficient translation (Fig. S6). In addition, proteomic profiling indicated a complete absence of detectable peptides encoded by exon 1 ($P = 3.6 \times 10^{-9}$ when compared with same-batch controls).

Patient 2: 16p13.3 Duplication-Triplication

The second patient, a 22-year-old woman, had a clinical history of mild intellectual disability, gait abnormalities, generalized dystonia, and parkinsonism. Further details are available in the Supporting Information Results.

Copy-number variant (CNV) analysis of trio ES data identified a possible candidate de novo heterozygous copy number gain of ~832 kb at the 16p13.3 locus (chr16:g.1765013_2597766dup) (Fig. 2A); however, the precise nature, boundaries, and internal architecture of the variant could not be resolved by short-read data. Given that cxSVs affecting this region have recently been associated with movement disorders,[22] ONT-based lrGS was performed to verify the presence and refine the structural properties of the ambiguous CNV detected by ES (Fig. 2B). This analysis showed a complex genomic rearrangement characterized by a large-scale duplication encompassing an internal, smaller-scale triplicated segment, structurally analogous to the variants described recently in the context of pathogenic 16p13.3 SVs[22] (Figs. 2C and S7). Nevertheless, precise breakpoint delineation and full resolution of the variant's internal architecture also remained unachievable by ONT pipeline analysis, owing to the exceptional repetitive complexity of the region and the disproportionate size of the cxSV relative to the mean read length generated. Through manual inspection of soft-clipped reads, the telomeric breakpoint of the duplicated segment was precisely mapped to chr16:g.1764458, with the soft-clipped sequences originating downstream of chr16:g.2351916, thereby defining the telomeric boundary of the triplicated segment (Fig. S7). The centromeric breakpoint of the triplication could not be precisely resolved because of the presence of a segmental duplication within the reference sequence, mirroring the challenges previously described.[22] Through manual review of read depth and allele fraction distributions at informative polymorphic sites, the proximal boundary of the triplication was estimated to lie between chr16:g.2580660 and chr16:g.2610716, with the former position considered more probable. Similarly, the distal breakpoint of the duplication could only be approximated between chr16:g.2634578 and chr16:g.2687070. The orientation of the most proximal segment of the duplication also remained undetermined. The triplicated segment encompassed the *ATP6V0C* locus, previously identified as the primary phenotype-driving gene in palindrome-mediated 16p13.3 triplications.[22] Notably, the broader SV additionally involved several genes with established relevance to other neurological and movement disorders, including *MAPK8IP3* (MIM *605431), *TSC2* (MIM *191092), and *CCNF* (MIM *600227), for which it cannot be excluded that a dosage imbalance may contribute to determining the patient's phenotype. A summary of affected genes and their predicted copy-number dosage is provided in Table S2.

Discussion

The two cases presented in this report exemplify both the diagnostic promise and the practical constraints of long-read sequencing in a real-world clinical setting. In the first patient, the additional integration of transcriptomic and proteomic analyses further illustrates how multi-omic profiling can yield unexpected yet diagnostically critical insights that would remain inaccessible through genomic approaches alone.

In the first patient with *PANK2*-related NBIA, the complementary application of srRNAseq and srWGS provided converging but individually inconclusive evidence. Critically, lrGS was required to confirm the presence and architecture of the pathogenic homozygous inversion and delineate the AluY-mediated NHAR mechanism, findings that an automated pipeline failed to produce despite including the two best-performing SV callers in the field.[25] Without prior clinical suspicion guiding manual inspection, the diagnosis would have been missed.

Beyond variant detection, the subsequent multi-omic profiling demonstrated a level of molecular complexity that was neither anticipated from the genomic data nor fully reconciled across analytical layers, because neither RNA outlier analysis nor proteomics alone accurately reflected the underlying biological reality, namely, a homozygous truncating rearrangement with complete loss of wild-type protein. Conversely, a DNA-only approach would not have shown the unexpected abundance and diversity of residual truncated isoforms, whose functional significance and potential contribution to the phenotype remain to be determined, even though the clinical severity suggests a near-complete loss of PANK2 function; targeted activity assays may shed more light on this aspect.[26] Our observations suggest that hard-to-predict splicing events (even involving

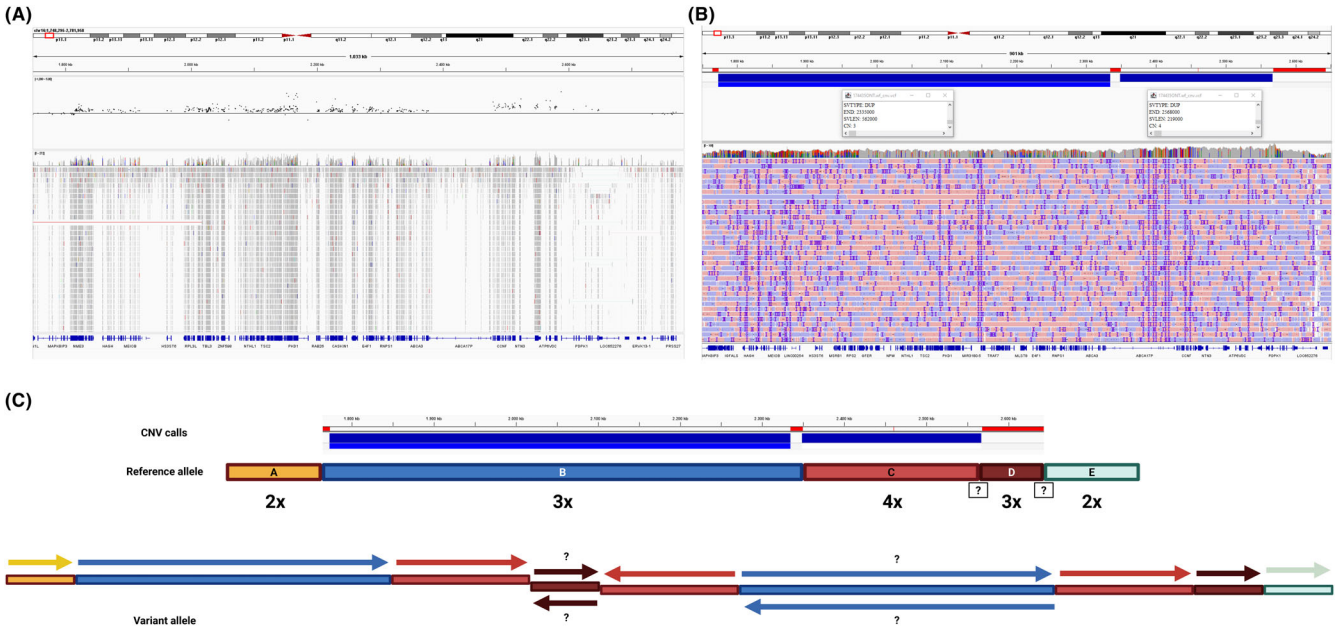

FIG. 2. Genomic characterization of the heterozygous de novo 16p13.3 duplication-triplication in patient 2. (**A**) Integrative Genomics Viewer (IGV) visualization of exome sequencing (ES) data displaying read-depth coverage across the relevant 16p13.3 genomic region, as estimated by ExomeDepth.[24] An elevated read-depth signal consistent with a heterozygous copy-number gain of ~832 kb was detected; however, the internal architecture and precise boundaries of the variant could not be resolved. (**B**) IGV visualization of ONT long-read genome sequencing (lrGS) read alignments across the same region. Colored bars above the reads indicate automated copy-number variant (CNV) calls generated by the lrGS pipeline, representing the estimated duplicated segment (upper dark blue and lower light blue) and triplicated segment (upper dark blue and lower white). Red bars were added manually following direct inspection of the read-depth profiles and soft-clipped read data, and indicate a more accurate delineation of the boundaries of the CNV segments. Two distinct duplication calls were returned by the automated pipeline, corresponding to the duplicated and triplicated tiers of the rearrangement, respectively. (**C**) Schematic representation of the interpreted 16p13.3 structural rearrangement. The reference allele is depicted as five discrete genomic segments (A–E). Estimated allelic dosage for each segment is indicated as 2× (diploid), 3× (triplicated), or 4× (quadruplicated), with 2× representing the wild-type copy number. Framed question marks denote breakpoints that could not be precisely resolved. Arrows indicate the estimated orientation of each segment relative to the forward strand of the reference allele; segments accompanied by unframed question marks had orientations that could not be unambiguously determined from the available data. [Color figure can be viewed at wileyonlinelibrary.com]

different loci) or posttranscriptional regulatory mechanisms may modulate residual *PANK2* output in ways that current predictive frameworks cannot anticipate, and underscore the indispensability of lrRNAseq in resolving transcript-level complexity that short-read approaches misrepresent.

In the second patient with 16p13.3 duplication-triplication, lrGS successfully identified the internal triplicated segment nested within the larger duplication, a tier of structural complexity entirely unappreciated by ES. Read-depth profiles were also more reliably interpretable in long-read data, and manual inspection of soft-clipped reads enabled precise mapping of the telomeric breakpoint of the duplication and the boundary between the duplicated and triplicated segments. However, even with sequencing depth substantially exceeding that reported in prior studies of this locus,[22] the centromeric breakpoints remained unresolvable because of a flanking segmental duplication in the reference sequence, a limitation previously noted by Fasham et al.[22] Full resolution of such regions would likely require ultra-long read lengths in the order of hundreds of kilobases, which is currently beyond the routine output of available platforms. This finding directly challenges the premise that contemporary long-read sequencing kits can serve as a universal single-test solution for cxSV characterization.[27]

Across both cases, a unifying theme emerges: the diagnostic resolution of cxSVs currently depends critically on expert-guided manual curation at different analytical levels. Automated pipelines, whether short- or long-read based, fell short in detecting, characterizing, or correctly interpreting more complex variants and their molecular consequences. This represents a substantial obstacle to the scalable implementation of long-read sequencing and multi-omic diagnostics in routine clinical practice and highlights the urgent need for more robust, SV-aware automated tools capable of handling complex rearrangements in repetitive genomic contexts.

This study had limitations. First, transcriptomic and proteomic analyses were performed in only one of the two patients, limiting the generalizability of the multi-omic observations. Although fibroblast-based srRNAseq has been shown to capture more than 80% of the transcriptional landscape of dystonia-associated and other neurological disease–associated genes,[20] expression studies involving neurologically relevant

isoforms would benefit from tissue-specific analyses.[28] In addition, the limited sample size of this study precludes definitive conclusions; this work is intended as an illustrative contribution. Systematic expansion of the case series will be necessary to establish a more generalizable understanding of the capabilities and limitations of long-read and multi-omic approaches for cxSV diagnostics.

Conclusions

The two cases presented in this report illustrate that long-read sequencing and multi-omic analyses hold considerable potential for uncovering and characterizing cxSVs that elude conventional short-read approaches. However, accurate interpretation of genomic variants and their molecular consequences required complementary expert-guided manual curation, because automated tools across used platforms typically failed to detect or fully resolve the identified rearrangements. Careful, integrative, and critically informed analysis by specialists therefore remains indispensable, representing a bottleneck on the path toward scalable, automated diagnostic pipelines for cxSVs.

Author Roles: Conceptualization, U.S. and M.Z. Data curation, U.S., M.P., R.K., A.S., S.L., C.L., M.A., J.M., E.G. Investigation, U.S., M.P., M.B., I.D., P.H., S.L., K.D., A.I., M.M.-B., D.W., M.S., K.K.-S., T.H., T.B., E.G. Software, M.P., A.S. Writing – original draft preparation, U.-S. and M.Z. Writing – review and editing, M.Z. Visualization, U.S. and M.Z. Supervision, H.P., J.W., M.K., M.Z. Project administration, J.W. and M.Z. All authors read and approved the final manuscript.

Acknowledgments: We thank the patients and their families for their participation in this study. We thank Katharina Eyring, Katharina Mayerhanser, Nicola Plathner, and Silke Slanz for excellent technical assistance. M.Z. is a member of the Medical and Scientific Advisory Council of the Dystonia Medical Research Foundation and a member of the Governance Council of the International Cerebral Palsy Genomics Consortium. BioRender was used to create (parts of) the figures in this report (https://www.biorender.com). Open Access funding enabled and organized by Projekt DEAL.

Financial Disclosures and Conflicts of Interest: Author disclosures are available in the Supporting Information.

Data Availability Statement

The data that support the findings of this study are available from the corresponding author upon reasonable request.

References

1. Perez-Duenas B, Gorman K, Marce-Grau A, et al. The genetic landscape of complex childhood-onset hyperkinetic movement disorders. Mov Disord 2022;37(11):2197–2209. https://doi.org/10.1002/mds.29182
2. Lange LM, Gonzalez-Latapi P, Rajalingam R, et al. Nomenclature of genetic movement disorders: recommendations of the International Parkinson and Movement Disorder Society task force - an update. Mov Disord 2022;37(5):905–935. https://doi.org/10.1002/mds.28982
3. Indelicato E, Zech M, Eberl A, et al. Insights on the shared genetic landscape of neurodevelopmental and movement disorders. Curr Neurol Neurosci Rep 2025;25(1):24. https://doi.org/10.1007/s11910-025-01414-w
4. Alvarez-Mora MI, Rodriguez-Revenga L, Jodar M, et al. Implementation of exome sequencing in clinical practice for neurological disorders. Genes (Basel) 2023;14(4):813. https://doi.org/10.3390/genes14040813
5. Tenorio RB, Camargo CHF, Donis KC, Almeida CCB, Teive HAG. Diagnostic yield of NGS tests for hereditary ataxia: a systematic review. Cerebellum 2024;23(4):1552–1565. https://doi.org/10.1007/s12311-023-01629-y
6. Penn D, Amir Y, David GB, et al. High genetic diagnostic yield for patients with rare movement disorders at a single-center neurogenetics clinic. Mov Disord Clin Pract 2025;12(11):1811–1820. https://doi.org/10.1002/mdc3.70145
7. Zech M, Jech R, Boesch S, et al. Monogenic variants in dystonia: an exome-wide sequencing study. Lancet Neurol 2020;19(11):908–918. https://doi.org/10.1016/S1474-4422(20)30312-4
8. Kosugi S, Terao C. Comparative evaluation of SNVs, indels, and structural variations detected with short- and long-read sequencing data. Hum Genome Var 2024;11(1):18. https://doi.org/10.1038/s41439-024-00276-x
9. Marwaha S, Knowles JW, Ashley EA. A guide for the diagnosis of rare and undiagnosed disease: beyond the exome. Genome Med 2022;14(1):23. https://doi.org/10.1186/s13073-022-01026-w
10. Park KJ, Lee W, Chun S, Min WK. The frequency of discordant variant classification in the human gene mutation database: a comparison of the American College of Medical Genetics and Genomics Guidelines and ClinVar. Lab Med 2021;52(3):250–259. https://doi.org/10.1093/labmed/lmaa072
11. Drost M, Dekker J, Ferraro F, et al. Routine RNA-based analysis of potential splicing variants facilitates genomic diagnostics and reveals limitations of in silico prediction tools. HGG Adv 2026;7(1):100521. https://doi.org/10.1016/j.xhgg.2025.100521
12. Pejaver V, Byrne AB, Feng BJ, et al. Calibration of computational tools for missense variant pathogenicity classification and ClinGen recommendations for PP3/BP4 criteria. Am J Hum Genet 2022;109(12):2163–2177. https://doi.org/10.1016/j.ajhg.2022.10.013
13. Moustakli E, Zagorianakou N, Makrydimas S, Miltiadous A, Tzallas AT, Makrydimas G. Beyond the exome: the role of noncoding and regulatory variants in monogenic diseases. Curr Issues Mol Biol 2025;47(12):1038. https://doi.org/10.3390/cimb47121038
14. Hops W, Weiss MM, Derks R, et al. HiFi long-read genomes for difficult-to-detect, clinically relevant variants. Am J Hum Genet 2025;112(2):450–456. 10.1016/j.ajhg.2024.12.013
15. Lunke S, Bouffler SE, Patel CV, et al. Integrated multi-omics for rapid rare disease diagnosis on a national scale. Nat Med 2023;29(7):1681–1691. https://doi.org/10.1038/s41591-023-02401-9
16. Smirnov D, Konstantinovskiy N, Prokisch H. Integrative omics approaches to advance rare disease diagnostics. J Inherit Metab Dis 2023;46(5):824–838. https://doi.org/10.1002/jimd.12663
17. Yepez VA, Gusic M, Kopajtich R, et al. Clinical implementation of RNA sequencing for mendelian disease diagnostics. Genome Med 2022;14(1):38. https://doi.org/10.1186/s13073-022-01019-9
18. Sorrentino U, Pavlov M, Mirza-Schreiber N, et al. Integrating long-read nanopore sequencing for precision resolution of genomic variants in dystonia. Mov Disord 2026;41(1):70–83. https://doi.org/10.1002/mds.70072
19. Zech M, Dzinovic I, Skorvanek M, et al. Combined genomics and proteomics unveils elusive variants and vast aetiologic heterogeneity in dystonia. Brain 2025;148(8):2827–2846. https://doi.org/10.1093/brain/awaf059
20. Saparov A, Dzinovic I, Brunet T, et al. Fibroblast transcriptomics in molecular diagnostics of a comprehensive dystonia cohort. Ann Neurol 2026;99(6):1363–1378. https://doi.org/10.1002/ana.78171
21. Cogan G, Daida K, Blauwendraat C, et al. Exploration of neurodegenerative diseases using long-read sequencing and optical genome mapping technologies. Mov Disord 2025;40(6):996–1008. https://doi.org/10.1002/mds.30151
22. Fasham J, Rankin J, Schot R, et al. Palindrome-mediated 16p13.3 triplications cause a recognizable neurodegenerative disorder with

ataxia. Am J Hum Genet 2026;113(1):221–233. https://doi.org/10.1016/j.ajhg.2025.11.011

23. Robinson JT, Thorvaldsdottir H, Winckler W, et al. Integrative genomics viewer. Nat Biotechnol 2011;29(1):24–26. https://doi.org/10.1038/nbt.1754
24. Plagnol V, Curtis J, Epstein M, et al. A robust model for read count data in exome sequencing experiments and implications for copy number variant calling. Bioinformatics 2012;28(21):2747–2754. https://doi.org/10.1093/bioinformatics/bts526
25. Helal AA, Saad BT, Saad MT, Mosaad GS, Aboshanab KM. Benchmarking long-read aligners and SV callers for structural variation detection in Oxford nanopore sequencing data. Sci Rep 2024;14(1):6160. https://doi.org/10.1038/s41598-024-56604-2
26. Werning M, Mullner EW, Mlynek G, et al. PKAN neurodegeneration and residual PANK2 activities in patient erythrocytes. Ann Clin Transl Neurol 2020;7(8):1340–1351. https://doi.org/10.1002/acn3.51127
27. Negi S, Stenton SL, Berger SI, et al. Advancing long-read nanopore genome assembly and accurate variant calling for rare disease detection. Am J Hum Genet 2025;112(2):428–449. https://doi.org/10.1016/j.ajhg.2025.01.002
28. Nicolas-Martinez EC, Robinson O, Pflueger C, et al. RNA variant assessment using transactivation and transdifferentiation. Am J Hum Genet 2024;111(8):1673–1699. https://doi.org/10.1016/j.ajhg.2024.06.018

Supporting Data

Additional Supporting Information may be found in the online version of this article at the publisher's web-site.